RSC Sustainability

ROYAL SOCIETY OF CHEMISTRY

PAPER

View Article Online
View Journal | View Issue

Cite this: *RSC Sustainability*, 2026, **4**, 851

Green extraction of cellulose fibers from pineapple crown waste for the development of pH-sensitive bioplastic films based on starch and purple cabbage anthocyanins

Nguyen Bui Anh Duy, [ab] Nguyen Thanh Huy, [ab] Bui Phuong Dong,[c] Pham Nguyen Hong Nhu,[c] Phan Quoc Phu *[ab] and Nguyen Chi Thanh *[c]

Environmental concerns over plastic waste and food safety have driven the development of smart and biodegradable active packaging materials. This study reports an intelligent bioplastic film capable of real-time monitoring of food freshness. Cellulose fibers (CFs) were extracted from pineapple crown waste through alkali and hydrogen peroxide treatment, followed by citric acid hydrolysis to enhance crystallinity. The extraction yield of cellulose fibers was 48.25 ± 0.37%, with a crystallinity index of 78.54%, confirming the effective removal of amorphous components. The obtained cellulose fibers were incorporated as reinforcing agents into cassava starch films containing a fixed amount of purple cabbage anthocyanin extract (2 mL, 255.49 mg L^{-1}). Mechanical analysis revealed that the optimal cellulose concentration was 16 wt%. The resulting intelligent bioplastic film exhibited an apparent color change from red to green or yellow, consistent with the behavior of an anthocyanin solution. During shrimp storage, the film functioned as a freshness indicator, changing color from purple to blue upon exposure to volatile amines such as trimethylamine (TMA), dimethylamine (DMA), and ammonia (NH_3). These findings demonstrate the potential of this intelligent biodegradable packaging for real-time food quality monitoring and environmental sustainability.

Received 5th August 2025
Accepted 2nd December 2025

DOI: 10.1039/d5su00648a

rsc.li/rscsus

Sustainability spotlight

This study addresses the pressing need for sustainable utilization of agricultural residues by transforming pineapple crown waste into high purity cellulose through an environmentally friendly citric acid process. The approach eliminates the use of strong mineral acids, thereby reducing chemical waste, corrosion risk, and water consumption. The recovered cellulose was applied to fabricate starch-based bioplastic films incorporated with purple cabbage anthocyanins, which function as color changing indicators under different pH conditions. This work represents a practical step toward green innovation in the valorization of biomass resources and the development of intelligent and biodegradable packaging materials. The study aligns with the United Nations Sustainable Development Goals 9 (Industry, Innovation and Infrastructure), 12 (Responsible Consumption and Production), and 13 (Climate Action).

Introduction

During storage, food products are highly susceptible to spoilage due to microbial growth and biochemical reactions such as lipid oxidation and protein degradation.[1] These processes generate volatile compounds, including ammonia (NH_3), trimethylamine (TMA), and organic acids, which cause fluctuations in the pH of the packaging environment.[2] Although packaging helps protect food from external influences, most current materials are synthetic plastics derived from petroleum.[3] These materials are not biodegradable and have the risk of chemical contamination in food, raising serious concerns for both human health and environmental sustainability.[4–6] To address these challenges, biodegradable intelligent packaging has emerged as a promising and sustainable solution.[7–9] Intelligent packaging not only offers physical protection but also integrates sensing capabilities to monitor and respond to biochemical changes occurring in food during storage.[10] Among various indicators, the pH was considered a critical parameter due to its direct correlation with food freshness. Therefore, pH-sensitive materials can be effectively employed as visual indicators in active packaging.[11]

[a]*Department of Polymer Materials, Faculty of Materials Technology, Ho Chi Minh City University of Technology (HCMUT), 268 Ly Thuong Kiet Street, Dien Hong Ward, Ho Chi Minh City, Vietnam. E-mail: nbaduy.sdh241@hcmut.edu.vn; nthuy.sdh241@hcmut.edu.vn; pqphu@hcmut.edu.vn*

[b]*Vietnam National University Ho Chi Minh City (VNUHCM), Thu Duc Ward, Ho Chi Minh City, Vietnam*

[c]*Faculty of Applied Sciences, Ho Chi Minh City University of Technology and Education, 01 Vo Van Ngan, Thu Duc Ward, Ho Chi Minh City, Vietnam. E-mail: 20130020@student.hcmute.edu.vn; 21130086@student.hcmute.edu.vn; thanhnc@hcmute.edu.vn*

Anthocyanins are natural pigments found in abundance in purple plants such as purple cabbage, butterfly pea flowers, and purple sweet potato, and they can change their structure in response to pH, resulting in distinct, visible color changes.[12–15] In acidic environments, anthocyanins appear red as the pH decreases, and the color changes to purple, blue, green, or yellow, depending on the degree of alkalinity.[16–18] However, to develop pH-responsive packaging films that are also mechanically stable and biodegradable, careful selection and combination of matrix materials is required.

Cassava starch is a natural polysaccharide widely available in Vietnam, known for its good film-forming ability and low cost.[19–21] Nevertheless, films made from pure starch typically exhibit poor mechanical strength and high moisture sensitivity.[22] Reinforcement with cellulose is therefore necessary to improve the film's durability and stability.[23] Among various cellulose-rich sources, pineapple crown waste – a common agricultural by-product in Vietnam – is considered a promising candidate for cellulose extraction.[24,25]

One significant challenge in utilizing cellulose is its extraction, which traditionally relies on strong mineral acids such as sulfuric or hydrochloric acid.[26–28] Although effective, these methods pose risks of environmental contamination and equipment corrosion and require complex neutralization steps.[29] According to recent studies, citric acid has demonstrated the ability to effectively remove lignin and hemicellulose while maintaining a high crystallinity index in the cellulose structure.[30,31] Moreover, this method generates minimal hazardous by-products, reduces the need for chemical neutralization, and consumes less water. With a moderate acidity of around pH 3.5, citric acid facilitates sufficient hydrolysis while preserving the structural integrity of the cellulose fibers. However, research on the application of citric acid for cellulose hydrolysis from agricultural residues in Vietnam remains scarce, particularly concerning pineapple crown waste. Previous studies have mainly applied this green hydrolysis approach to other biomass sources such as eucalyptus kraft pulp,[32] commercial microcrystalline cellulose,[33] bean husks,[34] and date palm residues.[35] Therefore, this study underscores the novelty, practical significance, and potential of this environmentally friendly extraction strategy for the efficient isolation of cellulose from pineapple crown waste.

Based on the above discussion, this study aims to develop an intelligent biodegradable packaging film capable of visually monitoring food freshness through pH-induced color changes. The material design integrates cellulose fibers extracted from pineapple crown waste, a largely unexplored agricultural by-product in Vietnam, using citric acid-assisted hydrolysis as a reinforcing agent, and anthocyanin extracted from purple cabbage as a natural pH-sensitive indicator within a cassava starch matrix. This approach addresses the limited research on eco-friendly cellulose extraction and the application of natural color indicators in starch-based films while valorizing agricultural waste. The outcomes of this study are expected to advance sustainable, intelligent food packaging systems, providing a multifunctional, environmentally friendly solution that aligns with circular economy principles.

Materials and methods

Materials

Materials. Pineapple crown waste (*Ananas comosus* L.) was collected from Tien Giang Province, Vietnam. Purple cabbage (*Brassica oleracea* var. *capitata* f. *rubra*) was obtained from Lam Dong Province, Vietnam. Cassava starch was purchased from Hiep Phat International Agricultural Co., Ltd, Tay Ninh, Vietnam, and contained 18.12 ± 0.07% amylose and 76.17 ± 0.04% amylopectin, which were determined using the method described in our previous study.[36] Sodium hydroxide (NaOH), hydrogen peroxide (H_2O_2), citric acid ($C_6H_8O_7$), potassium chloride (KCl), hydrochloric acid (HCl), sodium acetate (CH_3COONa), acetic acid (CH_3COOH), ethanol (C_2H_5OH), and glycerol ($C_3H_8O_3$) were purchased from Sigma Aldrich. Distilled water was used throughout the experiments.

Methods

Extraction of cellulose fibers (CFs) from pineapple crowns. The extraction process was designed with reference to earlier studies and adjusted to fit the objectives of this work.[33–35,37,38] The pineapple crowns were pretreated by washing, cutting into small pieces, drying at 50 °C for 24 hours, and grinding to obtain pineapple crown fibers (PCF). Then, the PCF were soaked in hot water at 100 °C to remove water-soluble compounds. Next, alkaline treatment was performed by soaking the raw material in 6% NaOH solution at 80 °C for 2 hours at a 1 : 20 (w/v) ratio to remove most of the hemicellulose and some of the lignin. After treatment, the samples were washed several times with distilled water until the pH was neutral, and then bleached with a 5% hydrogen peroxide (H_2O_2) solution at 80 °C for 2 hours. Finally, the obtained cellulose fibers were hydrolyzed with 60% citric acid at 90 °C for 6 hours to remove the amorphous regions. After hydrolysis, the samples were washed with distilled water until neutral and freeze-dried at −40 °C for 48 h. The schematic diagram in Fig. 1a shows the cellulose fiber extraction process.

Extraction of purple cabbage extract. The overall extraction procedures were developed based on previously reported methods with appropriate modifications.[39,40] After being cleaned, the purple cabbage was finely chopped and soaked in 50% ethanol at a 1 : 10 (w/v) ratio. The extraction was conducted in a tightly sealed glass container at 5 ± 2 °C for 24 hours to minimize anthocyanin degradation. After soaking, the mixture was filtered to remove solid residues, and the anthocyanin-containing extract was collected. The obtained extract was then concentrated using a rotary vacuum evaporator (Buchi R210, Switzerland; ID: RE-01HL) at 40 °C for about 2 hours to remove ethanol and part of the water, leaving 10% of the initial volume. The concentrated purple cabbage extract (PCE) was stored in dark glass bottles at 5 ± 2 °C until further use. A schematic diagram of the anthocyanin extraction process is illustrated in Fig. 1b.

Bioplastic film manufacturing. Cassava starch (2.5 g) was dispersed in distilled water at a ratio of 1 : 20 (w/v), followed by the addition of CFs at different concentrations of 0, 8, 16, and

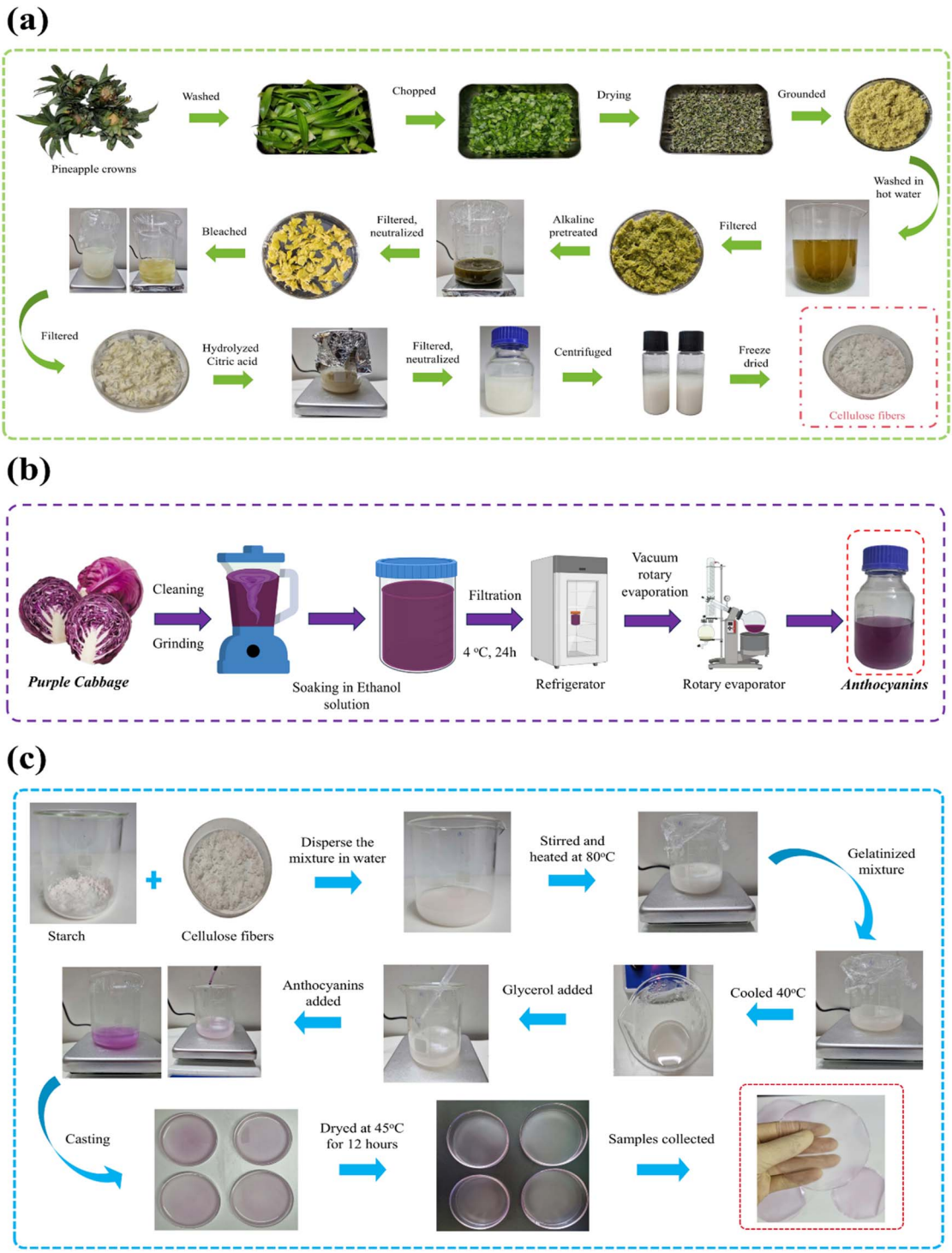

Fig. 1 Cellulose fiber extraction process (a), anthocyanin extraction process (b), and bioplastic film manufacturing process (c).

24 wt% (based on the weight of starch), and labeled as CS 0.0, CS 0.2, CS 0.4, and CS 0.6, respectively. The mixture was ultrasonicated for 15 min at room temperature, then stirred at 400 rpm and heated to 80 °C for 15 min to complete gelatinization. After cooling to 40 °C, 2 mL of anthocyanin extract and 30% glycerol (w/w based on starch) were added. The resulting mixture was stirred for an additional 10 min to ensure homogeneity. To ensure uniform film thickness across all samples, 25 mL of the homogeneous film-forming solution was poured into Petri dishes with a 10 cm diameter, and 20 mL into those with an 8 cm diameter, under identical conditions. The films were then dried at 45 °C for 12 h. A schematic illustration of the film preparation process is shown in Fig. 1c.

Characterization analysis

Extraction yield of CFs. The yield (H, %) of cellulose fiber extraction from pineapple crowns was calculated using eqn (1).[41] This analysis was repeated three times, and the average value was reported.

$$H(\%) = \frac{m_f}{m_i} \times 100 \quad (1)$$

where m_f is the mass of CFs (g) and m_i is the mass of dried pineapple crown fibers (g).

Moisture content. The moisture content of the CFs and the bioplastic films was determined by weighing the samples before and after drying at 105 °C until a constant weight was achieved. The moisture content (MC, %) was calculated as the percentage of weight loss relative to the initial sample weight, as expressed in eqn (2). The analysis was performed in triplicate, and the mean values were reported.

$$\text{MC } (\%) = \frac{W_1 - W_2}{W_1} \times 100 \quad (2)$$

where W_1 is the initial weight of the CFs or bioplastic films and W_2 is the weight of the CFs or bioplastic films after drying in the oven.

Scanning electron microscopy (SEM). The surface morphology of PCF and CFs was analyzed using field emission scanning electron microscopy (FESEM, S-4800, HITACHI, Japan) at the SHTP Research and Development Center, Saigon Hi-Tech Park, Vietnam. The samples were placed on carbon supports and coated with a thin platinum layer before observation. The average fiber diameter was determined from SEM images using ImageJ software by measuring at least 70 randomly selected fibers.

Fourier transform infrared (FTIR) spectroscopy. Fourier transform infrared (FTIR) spectra of PCF and CFs were analyzed using a NICOLET 6700 spectrometer (Thermo, USA) at the Institute of Applied Materials Science in Ho Chi Minh City, Vietnam. The spectral analysis was conducted over 4000 to 400 cm^{-1} with a resolution of 4 cm^{-1}, using a total of 64 scans. The samples were prepared as pellets by mixing the dried samples with KBr. This comprehensive analysis enables the identification of functional groups and provides insights into the chemical structure of the CFs and PCF.

X-ray diffraction (XRD). X-ray diffraction (XRD) analysis of PCFs and CFs was performed using an EMPYREAN diffractometer (PANalytical, the Netherlands). The instrument was operated at 40 kV and 45 mA, utilizing CuK_α X-ray radiation (wavelength = 0.1542 nm). Samples were analyzed over a 2θ scan range from 5° to 80°. The degree of crystallinity (DC, %) was quantitatively calculated using eqn (3).[42]

$$\text{DC } (\%) = \frac{A_c}{A_c + A_m} \times 100 \quad (3)$$

where A_c is the area of the crystalline region and A_m is the area of the amorphous region.

UV-vis analysis of PCE. The UV-vis spectrum of PCE was measured over the 380–760 nm range using a UV-vis spectrophotometer (JASCO V-730, Japan). The extract was obtained as a deep purple solution containing anthocyanins along with small amounts of co-extracted compounds such as sugars, organic acids, and polyphenols.[43] Buffer solutions used for pH adjustment were prepared following the procedure of Devarayan *et al.*[44] Specifically, hydrochloric acid–potassium chloride buffer at pH 2, citrate buffer at pH 3–6, phosphate buffer at pH 7–8, and carbonate–bicarbonate buffer at pH 9–10 were used. Under strongly alkaline conditions (pH 11–12), the pH was adjusted using appropriate mixtures of HCl and NaOH solutions. The pH value of PCE solution was subsequently adjusted from 2 to 12 using the corresponding buffer systems mentioned above. Each sample was analyzed in triplicate, and the average value was used for data analysis.

Anthocyanin content. Total monomeric anthocyanin (TMA) content was determined using the pH differential method described by Giusti *et al.*[45] The PCE was diluted with 0.025 M potassium chloride–hydrochloric acid buffer (pH 1.0) and 0.4 M sodium acetate–acetic acid buffer (pH 4.5) at a ratio of 1 : 9 (v/v). The sample was then fixed in a dark environment for about 30 minutes at room temperature, and its absorbance was measured at 520 and 700 nm using a UV-vis spectrophotometer. The relative absorbance of the purple cabbage extract was calculated using eqn (4).[46]

$$A = (A_{\lambda_{520}} - A_{\lambda_{700}})_{\text{pH 1.0}} - (A_{\lambda_{520}} - A_{\lambda_{700}})_{\text{pH 4.5}} \quad (4)$$

where $A_{\lambda_{520}}$ and $A_{\lambda_{700}}$ are the absorbance values measured at 520 and 700 nm, respectively; the subscripts pH 1.0 and pH 4.5 indicate measurements in buffer solutions at pH 1.0 and 4.5, respectively.

The total monomeric anthocyanin (TMA, mg L^{-1}) content in the extract was calculated using eqn (5).[46]

$$\text{TMA } (\text{mg L}^{-1}) = \frac{A \times \text{MW} \times \text{DF} \times 1000}{\varepsilon \times L} \quad (5)$$

where A is the relative absorbance, MW is the molecular weight of cyanidin-3-glucoside (449.2 g mol^{-1}), DF is the dilution factor, ε is the molar absorption coefficient (26 900 L mol^{-1} cm^{-1}), and L is the cuvette width (1 cm).

Solubility in water and moisture content of bioplastic films. The experiment was conducted according to the method described by Hailu *et al.*, with appropriate modifications.[39] Film samples (2 cm × 2 cm) were prepared from each formulation, and their thicknesses were measured before testing. The average thickness values were 0.092 ± 0.001 mm, 0.095 ± 0.002 mm, 0.098 ± 0.002 mm, and 0.104 ± 0.003 mm for CS 0.0, CS 0.2, CS 0.4, and CS 0.6, respectively. The measurements were performed at three different points on each film sample using an electronic thickness gauge (Mitutoyo 547-401A, Japan) with a resolution of 0.001 mm. The films were dried in an oven at 105 °C for three hours to determine the initial mass (W_3). After cooling in a desiccator, the samples were weighed accurately using an analytical balance. Next, the samples were soaked in 10 mL of deionized water in a 50 mL glass beaker at room temperature (approximately 25 ± 2 °C) for 24 h. After the soaking period, the solution containing the sample was filtered through a filter paper to collect the insoluble fraction. The

residue on the filter paper was carefully collected and dried in an oven at 105 °C for three hours until a constant mass was achieved. The dried sample was cooled in a desiccator and weighed to determine the residual mass (W_4). The water solubility (SW, %) of the bioplastic films was calculated according to eqn (6).[39] This analysis was performed in triplicate, and the average value was recorded.

$$\mathrm{SW}(\%) = \frac{W_3 - W_4}{W_3} \times 100 \quad (6)$$

Mechanical properties of bioplastic films. The mechanical properties of the bioplastic films were determined using a Shimadzu AGS-X tensile testing machine (Japan) at the Materials Technology Laboratory of Ho Chi Minh City University of Technology Education. The tensile test was conducted according to the international standard ASTM D882 at a test speed of 12.5 mm min^{-1}. The obtained films were then conditioned at 23 ± 2 °C and 50 ± 10% relative humidity for 48 h before mechanical testing. Ten replicate measurements were performed, and the average value was reported for evaluation. The tensile strength (TS, MPa) and elongation at break (EAB, %) were calculated using eqn (7) and (8), respectively.[39]

$$\mathrm{TS\ (MPa)} = \frac{F}{A} \quad (7)$$

where F (N) is the tensile force of the bioplastic films and A (mm^2) is the cross-sectional area of the bioplastic films.

$$\mathrm{EAB}(\%) = \frac{l_1 - l_0}{l_0} \times 100 \quad (8)$$

where l_o (mm) is the initial length of the bioplastic films and l_1 (mm) is the length at the breaking point of the bioplastic film.

Young's modulus (E, MPa) is related to its tensile strength and elongation, as shown in eqn (9).[39]

$$E(\mathrm{MPa}) = \frac{\mathrm{TS}}{\mathrm{EAB}} \quad (9)$$

pH-sensitivity of the colorimetric indicator. The pH responsiveness of the anthocyanin extract was evaluated using the method described by Diksha Thakur *et al.*, with some necessary modifications.[47] Specifically, film samples measuring 2 cm × 2 cm were immersed in different pH buffer solutions for 1 min. After exposure, the samples' color changes were recorded with a digital camera and analyzed in relation to the medium's pH.

Color property analysis. The colorimetric method for the CS 0.4 smart biofilm sample was performed as described by Gao *et al.* and Pang *et al.*, with minor adjustments to suit the experimental conditions.[48,49] The CS 0.4 bioplastic film sample was cut into 2 × 2 cm squares, then immersed in 5 mL of buffer solution at pH 2–12 for 5 min to evaluate the biofilm's color sensitivity to changes in the environmental pH. After treatment, the film samples were removed and lightly dried on absorbent paper before measuring color with a CHN Spec CS-10 handheld colorimeter. The measurements were conducted under a D65 illuminant and a 10° observer, using an LED light source. The color parameters collected according to the CIELAB color system include:

L^*: lightness, values from 0 (black) to 100 (white),

a^*: red–green axis, in which positive values represent red and negative values represent green,

b^*: yellow–blue axis, in which positive values represent yellow and negative values represent blue.

To evaluate the degree of color change after pH treatment, the overall color difference (ΔE) was calculated using eqn (10):

$$\Delta E = \sqrt{(L^* - L_0)^2 + (a^* - a_0)^2 + (b^* - b_0)^2} \quad (10)$$

where L_0^*, a_0^*, b_0^* is the initial color value of the film (before pH treatment), and L^*, a^*, and b^* are the color values after treatment. Each sample was measured at three random locations to increase the precision and eliminate local errors. This measurement enables accurate quantification of biofilm color changes across different pH environments.

Application of films as a pH indicator for food. To visually evaluate the color indicator ability of the bioplastic film CS 0.4 in food preservation, a typical experiment was conducted to monitor food freshness at room temperature. The food sample selected for testing was shrimp, which was purchased from Thu Duc market, Ho Chi Minh City, Vietnam. A sample of bioplastic film, cut into approximately 2 cm × 2.5 cm, was placed next to the food and covered with a plastic wrap for several hours to observe the color change, as described by Konala Akhila *et al.*[50]

Statistical analysis. All experiments were performed in triplicate, and the results were expressed as mean ± standard deviation (SD). The obtained data were processed using OriginPro 2018 (OriginLab Corporation, USA). The significant differences in the mean values were determined by one-way ANOVA followed by the Tukey test at the significance level of $p < 0.05$.

Results and discussion

Extraction yield of CFs

The extraction yield of cellulose fibers from PCF was 48.25 ± 0.37%, calculated according to eqn (1). This value was higher than those reported for other biomass sources such as corn cob (37.15%),[51] wheat straw (36.1%),[52] aloe peel (32%),[53] and rice husk (30%),[54] all of which were processed through acid hydrolysis with inorganic acids. These results confirm that the sequential treatment with NaOH and H_2O_2, followed by citric acid hydrolysis, provides an effective route for cellulose recovery from pineapple crown waste.

Although the yield obtained in this study was lower than that reported by Fitriani *et al.* for cellulose fibers extracted from the same raw material, pineapple crown fibers (76.23%),[55] this difference cannot be explained solely by variations in the original biomass source. It also reflects the distinct extraction and purification strategies adopted. In the above study, a one-step combined treatment using sodium hydroxide (NaOH) and hydrogen peroxide (H_2O_2) was applied to the pineapple crown fibers for 1 hour before hydrolysis with 3 M sulfuric acid (H_2SO_4) at 45 °C. This procedure is known to accelerate the removal of

amorphous domains and enhance cellulose recovery, though it may be less effective in eliminating hemicellulose and lignin residues. In contrast, the present study employed separate alkaline and bleaching treatments, each conducted for two hours at 80 °C, to ensure more thorough delignification and dehemicellulization, both of which account for a large proportion of pineapple crown fiber biomass.[28,56] Before hydrolysis with 60% w/w citric acid at 90 °C for six hours, this process enhances the removal of impurities while preserving the structural integrity of cellulose; however, the repeated washing steps required to remove residual chemicals can lead to partial cellulose loss, resulting in a lower overall extraction yield.

Compared with other studies employing citric acid as a green hydrolyzing agent, the extraction yield obtained in this work falls within the expected range for organic acid hydrolysis. Specifically, Aisy *et al.* reported the extraction of cellulose nanofibrils (CNFs) from date by-products that had undergone NaOH and H_2O_2 pretreatments, followed by hydrolysis with 5.5 M citric acid (approximately 80% w/w) at 100 °C for 6 h under ultrasonic assistance, achieving a yield of 51.73%.[35] Similarly, Hui Ji *et al.* utilized pre-bleached bagasse as the feedstock and conducted hydrolysis with 80% w/w citric acid at 100 °C for 4 h, resulting in a CNF yield of 63.4%.[38] The slightly lower yield observed in the present study can be attributed to the absence of ultrasonic enhancement and the adoption of milder hydrolysis conditions (60% w/w citric acid, 90 °C, 6 h), which were deliberately selected to minimize cellulose degradation while maintaining a practical balance between the recovery yield and economic feasibility. Overall, these findings substantiate that citric acid hydrolysis represents a sustainable and effective alternative to mineral acids for cellulose extraction from pineapple crown waste.

Moisture content of CFs

The moisture content of cellulose fibers extracted from pineapple crowns was determined using eqn (2).[57] The analysis yielded an average moisture content of 11.47 ± 0.58%.

Scanning electron microscopy

The morphological changes on the surface of PCF and CFs were analyzed by scanning electron microscopy, as illustrated in Fig. 2. As shown in Fig. 2a and b, PCF had a rough surface, and the cellulose chains tended to aggregate into fiber bundles. This behavior was attributed to the presence of compounds such as lignin, hemicellulose, pectin, and other non-cellulose substances, which acted as binders.[58] In contrast, the CFs observed in Fig. 2c and d have a well-defined fibrous structure with a smooth and uniform surface. These findings indicated that chemical treatment, especially hydrolysis with citric acid, effectively removed amorphous impurities.[59] The CFs had an average diameter in the range of 4.21–5.18 μm, as shown in Fig. 3. Compared with the study of Kassim *et al.*, the cellulose fibers were extracted from the same plant source through hydrolysis with H_2SO_4, and the average fiber diameter was 3.66 μm, which is relatively close to the value reported in this study.[60] This indicates the potential of using citric acid as an adequate replacement for H_2SO_4 to reduce its environmental impacts.

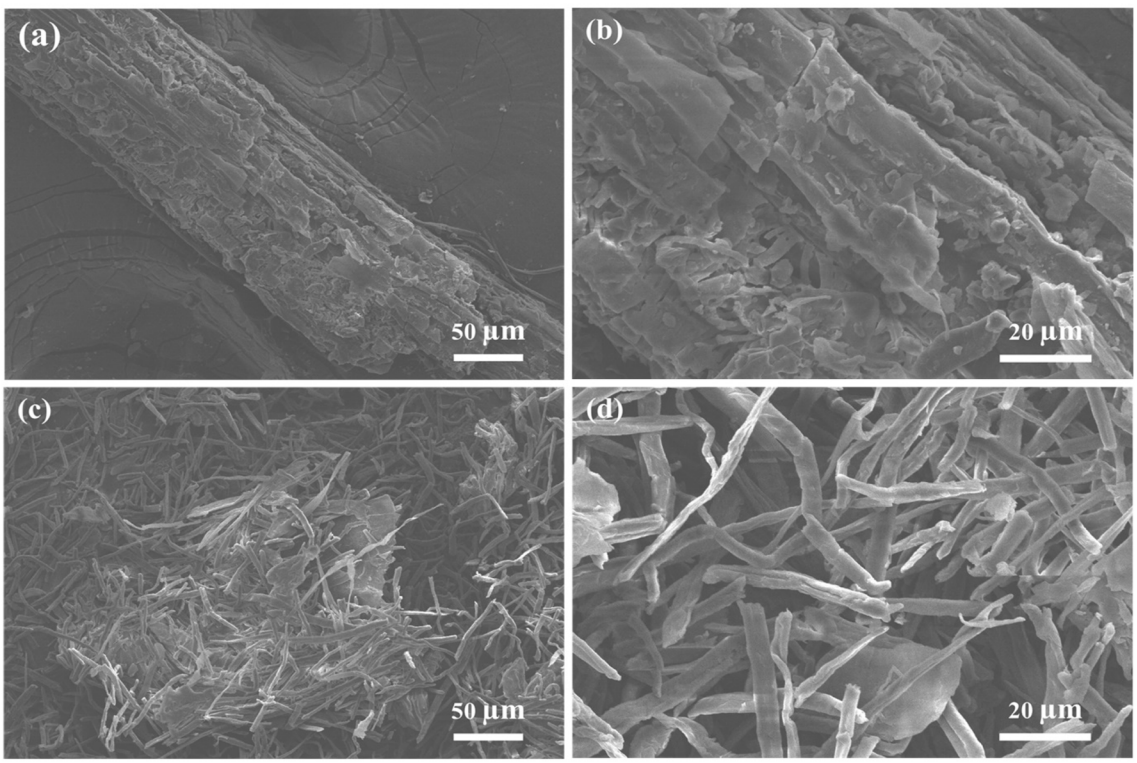

Fig. 2 SEM images of (a and b) fibers from pineapple crown waste at ×300 and ×1000 magnification, respectively, and (c and d) obtained cellulose fibers at ×300 and ×1000 magnification, respectively.

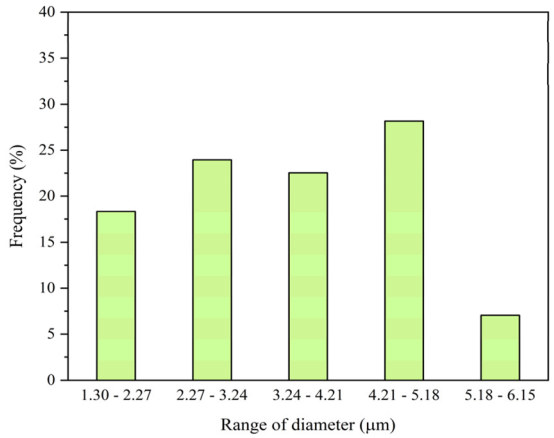

Fig. 3 Diameter distribution of CFs.

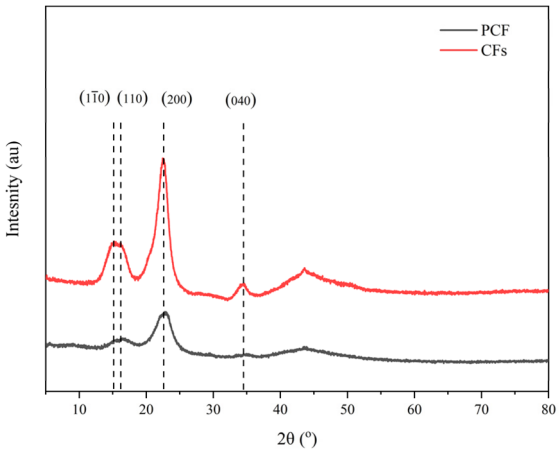

Fig. 5 XRD patterns of PCF and CFs.

Fourier transform infrared spectroscopy

The FTIR spectra of PCF and CFs are shown in Fig. 4. The absorption bands in the range of 3700–3000 cm^{-1}, with a maximum peak at approximately 3345 cm^{-1}, correspond to the stretching vibration of the hydroxyl group (O–H) present in the chemical structure of the cellulose molecule in both samples. The peaks observed at 2919 cm^{-1} and 1639 cm^{-1} are attributed to the stretching vibration of the C–H and O–H groups, respectively. Furthermore, the peak at 1740 cm^{-1} in the spectrum of PCF is assigned to the stretching vibration of the carbonyl group (C=O) in the chemical structure of hemicellulose, or from the ester bond of the carboxylic group in the chemical structure of lignin.[60] In addition, the absorption peaks at 1050 cm^{-1} and 892 cm^{-1} were assigned to the stretching vibration of the (C–O–C) bond in the pyranose ring and the glycosidic bond between glucose units in the cellulose chain. Interestingly, compared to the FTIR spectrum of PCF, the FTIR spectrum of CFs showed a decrease in absorption intensity at 1740 cm^{-1}, meaning that a part of the hemicellulose was removed. Furthermore, the disappearance of the peak at 1245 cm^{-1}, which is typically associated with syringyl-type lignin, was also not observed in the FTIR spectrum of the CFs,

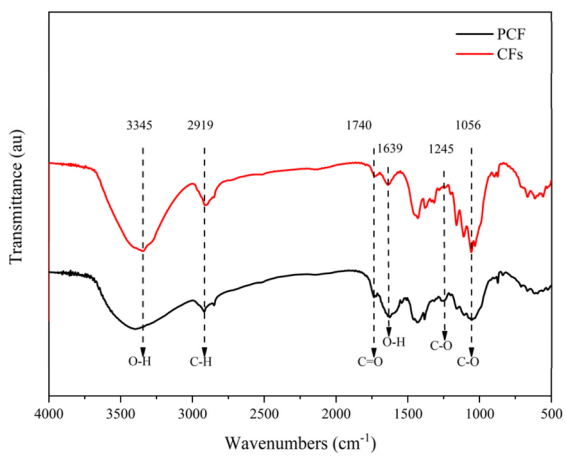

Fig. 4 FTIR spectra of PCF and CFs.

indicating that the chemical treatments significantly removed the amorphous components while preserving the chemical structure of the obtained cellulose fibers.[55]

X-ray diffraction

The X-ray diffraction patterns of the PCF and CFs are shown in Fig. 5. The results showed that both PCF and CFs exhibited characteristic diffraction peaks at 2θ values of approximately 15.2°, 16.1°, 22.6° and 34.6°, corresponding to the (1$\bar{1}$0), (110), (200) and (040) crystal planes, respectively, representing the structure of type I cellulose.[61] In addition, the crystallinity index of CFs calculated from eqn (3) was 78.54%, which was significantly higher than that of PCF (36.41%). This indicated that the chemical treatments, especially citric acid hydrolysis, effectively removed amorphous components such as hemicellulose, lignin, and other non-cellulose substances, thereby increasing the crystallinity of the CFs.[62] These results are consistent with those reported by Diana Choquecahua Mamani *et al.*[63]

Crystallinity was considered a critical parameter that determined many mechanical and physicochemical properties of cellulose-based materials. Fig. 6 visually illustrates the crystallinity of the CFs in this study in comparison with previously reported values for cellulose hydrolyzed from various biomass sources using inorganic acids.[54,55,60,64–70] This result indicated that, although citric acid was weaker in acidity compared to H_2SO_4 and HCl, it was still able to disrupt amorphous and paracrystalline regions within the cellulose structure when suitable hydrolysis conditions were applied. The variation in crystallinity among samples was influenced not only by the type of acid used but also by the microstructure of the raw biomass, fiber size, the initial ratio of crystalline to amorphous regions, and specific treatment parameters.[71] Achieving a high degree of crystallinity using an organic acid demonstrated the effectiveness and sustainability of the proposed method compared to conventional inorganic acid-based processes.

UV-vis analysis of PCE

The UV-vis absorption spectra of PCE at pH values ranging from 2 to 12 are shown in Fig. 7, showing distinct changes in both the

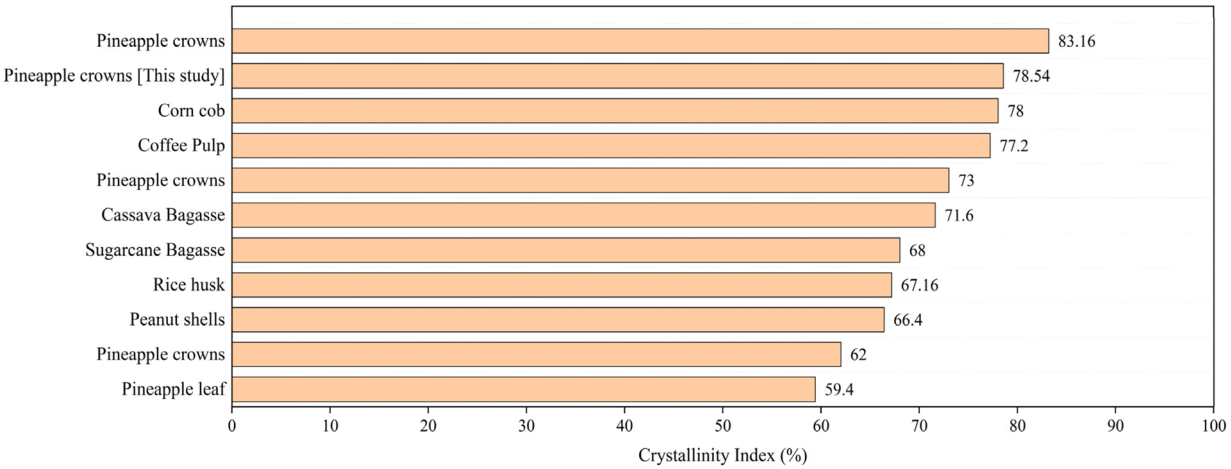

Fig. 6 Crystallinity index of CFs compared across biomass sources.

position and intensity of the absorption peaks. These changes reflected the characteristic structural transformations of anthocyanins under varying pH conditions. In the acidic medium (pH 2 to 4), a strong absorption peak at approximately 524 nm was observed, corresponding to the flavylium cation form. This form exhibited a deep red color and was considered the most stable under low pH conditions.[72] As the pH was increased to near-neutral levels (pH 5–6), the absorbance at approximately 524 nm decreased significantly. This reduction was attributed to the structural conversion of anthocyanins into colorless forms, such as carbinol bases and chalcones, which showed weak or negligible absorption in the visible region.[73] When the pH was further increased to alkaline conditions (pH 8 to 12), the absorption maximum shifted to a longer wavelength (600 to 620 nm). This shift was interpreted as resulting from the formation of quinonoid anion species or degradation products exhibiting blue or green coloration.[74] However, the absorbance at high pH values was markedly decreased, indicating that anthocyanins degraded or became less stable under alkaline conditions.[75] These results confirmed the pH sensitivity of anthocyanins and suggested their potential as natural indicators in innovative packaging.

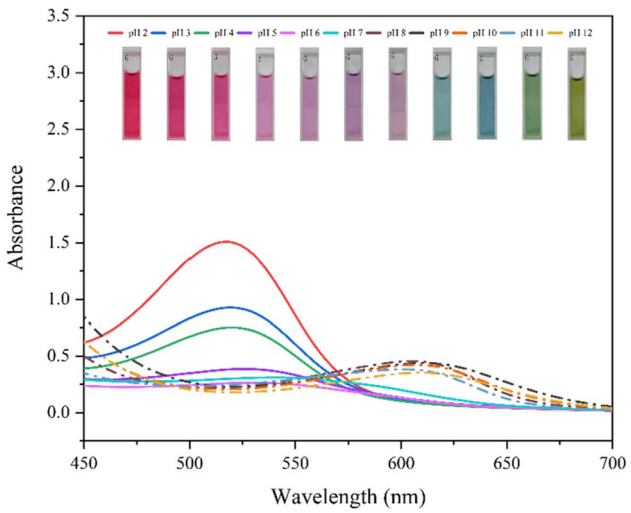

Fig. 7 UV-vis spectra of PCE in different pH buffer solutions.

Anthocyanin content

The UV-vis spectra of PCE at pH 1 and 4.5 are presented in Fig. S1. The total anthocyanin concentration extracted from purple cabbage using ethanol solvent was calculated using eqn (4) and (5) as 255.49 mg L^{-1}. Compared to other studies related to the anthocyanin concentration obtained from purple cabbage, this value is lower than that of Abderrahim Bouftou *et al.* (790.69 mg L^{-1}),[76] while it is higher than the value reported by Mohammad Shayan *et al.* (154 mg L^{-1}).[40] The difference in anthocyanin content can be attributed to several factors, including species, growth period, growing conditions, season, soil, and geographical origin, as well as different cultivation and extraction methods.[76]

pH-sensitivity of the colorimetric indicator

The pH sensitivity of the color indicator was evaluated by adding a fixed amount of PCE to buffer solutions with different pH values and to PCE-containing film samples. Fig. 8 shows that the pH-induced color changes in the observed film samples followed a similar trend to PCE. This result suggests that the fabricated bioplastic film has potential application as a pH sensor indicator in the field of innovative packaging. The color changes observed with increasing pH include purple or dark red in acidic environments, fading to red as the pH approaches neutral, and turning green or yellow in alkaline environments. These color change characteristics are consistent with the results reported by Alizadeh-Sani *et al.*[77]

Solubility in water and moisture content of bioplastic films

Water solubility and moisture content are two critical indicators for evaluating the stability of bioplastic films in humid environments, as they directly affect the mechanical properties and performance of the indicator film during use. The results presented in Table 1 show that the CS 0.0 film has the highest water solubility (22.74 ± 1.47%) and moisture content (18.35 ±

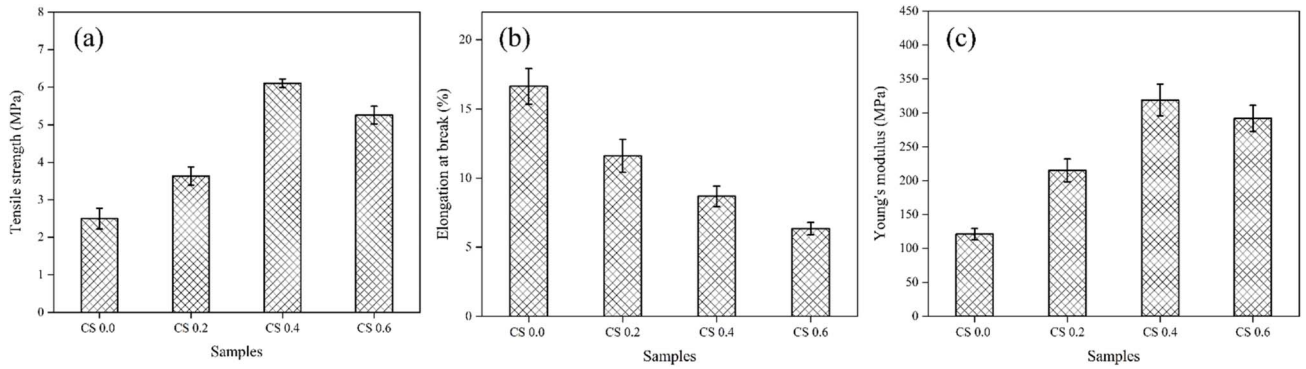

Fig. 8 (a) Tensile strength, (b) elongation at break and (c) Young's modulus of bioplastic film samples.

Table 1 Water solubility and moisture content of the bioplastic films[a]

Film samples	Solubility in water (%)	Moisture contents (%)
CS 0.0	22.74 ± 1.47[a]	18.35 ± 1.26[a]
CS 0.2	17.24 ± 0.96[b]	12.92 ± 1.12[b]
CS 0.4	16.83 ± 1.12[b]	12.28 ± 0.84[b]
CS 0.6	16.35 ± 1.28[b]	12.52 ± 1.04[b]

[a] Different superscripts in the column indicate significant differences between bioplastic films at p <0.05.

1.26%), reflecting its strong hydrophilicity and weakening of the polymer network due to the hydroxyl-rich structure of starch and glycerol.[78] This makes it susceptible to degradation in aqueous environments and is mechanically unstable. However, when CFs were added in increasing proportions (CS 0.2, CS 0.4, and CS 0.6), both solubility and moisture content were significantly reduced. This demonstrates that cellulose fibers play an essential role in reinforcing the polymer network through hydrogen bonding with the hydroxyl groups of starch and the phenolic functional groups of anthocyanins, thereby reducing the water contact space and limiting water absorption and retention capacity. This trend is consistent with previous studies.[79–81] It suggests the potential application of pH indicator films with good water resistance for packaging high-moisture foods such as fresh meat, seafood, pre-cut fruits, and dairy products.

Mechanical properties of bioplastic films

Fig. 9 and S2 show the mechanical properties of starch-based bioplastic films reinforced with the CFs and anthocyanins from purple cabbage. The results showed that both the tensile strength and Young's modulus of the films increased significantly with the addition of CFs, reaching the highest value at a concentration of 16 wt% (CS 0.4). At this concentration, the tensile strength reached 6.11 ± 0.12 MPa. At the same time, the Young's modulus increased to 318.96 ± 23.24 MPa, approximately 2.7 times higher than that of the unreinforced sample (CS 0.0), reflecting the improvement in both the tensile strength and stiffness of the material. This mechanical improvement is explained by the relatively good dispersion of cellulose fibers in the starch matrix, which promotes the formation of hydrogen bonds between the phases and helps transfer stress effectively.[82] However, when the CF concentration increased to 24 wt% (CS 0.6), the tensile strength tended to decrease slightly. The reason may be that the addition of high CF content hindered the interaction between starch molecules, leading to agglomeration and affecting the uniformity of the film.[83]

In contrast, the elongation at break gradually decreased with increasing CF content, indicating that the material became more brittle. Specifically, the CS 0.0 sample had an elongation at break of about 16.63 ± 1.28%, whereas the CS 0.6 sample showed a sharp decrease to about 6.48 ± 0.45%. This implies that at high concentrations, CFs reduced the flexibility of

Fig. 9 Color changes of PCE in different pH environments.

polymer chains, thereby reducing the film's elastic deformation capacity under tensile force. Overall, the CS 0.4 sample exhibited the best mechanical properties, suggesting potential applications in biodegradable packaging.

Color property analysis

The variation in L^*, a^*, and b^* values clearly reflected the color transition of the CS 0.4 bioplastic film under different pH conditions (Table 2), which was associated with transformations among key anthocyanin molecular structures, including the flavylium cation, quinoidal base, carbinol base, and chalcone. In strongly acidic media (pH 1–3), anthocyanins predominantly existed in the flavylium cation form, characterized by an intense purplish-red color, as indicated by very high a^* values (35.31–29.91) and slightly positive b^* values (4.99–9.78). Simultaneously, the low L^* values (44.84–54.84) suggested dark tones and high light absorption. As the pH increased to the neutral range (pH 4–7), anthocyanins transformed from the flavylium form to unstable intermediates, such as the carbinol base (colorless) and the quinoidal base (purple-blue).[84] This was reflected by a sharp decrease in a^*, a shift of b^* to negative values, and an increase in L^*, reaching a peak at pH 7 (71.90), which indicated a lighter color. From pH 8 to 10, anthocyanins mainly existed in the anionic quinoidal base form, resulting in blue to greenish hues, as evidenced by strongly negative a^* values (−4.87 to −9.97) and profoundly negative b^* values (−20.45 to −18.16).[85] Under strong alkaline conditions (pH 11–14), the anthocyanin structure was further transformed into the open-ring chalcone form, a more stable structure in alkaline environments, exhibiting intense yellow coloration. This was confirmed by significantly high positive b^* values (25.53–40.27) and slightly positive a^* values (2.25–5.35). These color changes are shown in Fig. S3.

The total color difference (ΔE) provided quantitative insight into the extent of color variation in the film under each pH conditions relative to its initial state.[85] Very high ΔE values at pH 1–3 (40.81–34.76) indicated drastic color changes when anthocyanins were mainly in the flavylium form. From pH 4 to 7, ΔE values decreased gradually and reached a minimum at pH 7 (2.43), indicating a color appearance closest to that of the untreated film. However, in alkaline environments (pH 8–14), ΔE significantly increased again, reaching the highest levels at pH 13 and 14 (55.49 and 53.54), due to the presence of yellow-colored chalcone or colorless degradation products. The observed color transitions across various pH levels demonstrated the high sensitivity and reliable color-sensing capability of the developed bioplastic film.

Application of films as a pH indicator for food

The color change of the bioplastic film reflects the quality deterioration of shrimp during storage, as shown in Fig. 10.

Table 2 Color parameters (L^*, a^*, and b^*) of the CS 0.4 bioplastic film sample[a]

Medium	Color response of films	L^*	a^*	b^*	ΔE
pH 1		44.84 ± 0.27^{k}	35.31 ± 0.87^{a}	4.99 ± 0.60^{e}	40.81 ± 0.94^{d}
pH 2		48.07 ± 0.35^{j}	32.36 ± 0.29^{b}	8.12 ± 0.79^{d}	38.72 ± 0.48^{e}
pH 3		54.84 ± 0.18^{i}	29.91 ± 0.57^{c}	9.78 ± 0.41^{d}	34.76 ± 0.11^{f}
pH 4		62.19 ± 0.23^{g}	25.15 ± 0.80^{d}	4.61 ± 0.87^{e}	25.31 ± 0.98^{h}
pH 5		65.76 ± 0.21^{e}	17.75 ± 0.92^{e}	-5.04 ± 0.43^{f}	12.75 ± 0.37^{j}
pH 6		70.16 ± 0.12^{c}	11.96 ± 0.81^{f}	-59.41 ± 0.48^{g}	5.06 ± 0.55^{l}
pH 7		71.90 ± 0.20^{b}	9.82 ± 0.91^{f}	-512.17 ± 0.76^{h}	2.43 ± 0.79^{m}
pH 8		75.00 ± 0.44^{a}	5.23 ± 0.58^{g}	-520.45 ± 0.49^{k}	9.22 ± 0.10^{k}
pH 9		64.87 ± 0.36^{f}	-54.87 ± 0.78^{i}	-514.9 ± 0.84^{i}	16.96 ± 0.70^{i}
pH 10		55.02 ± 0.19^{i}	-59.97 ± 0.64^{j}	-518.16 ± 0.67^{j}	$26.68 \pm 0.58^{g,h}$
pH 11		67.90 ± 0.24^{d}	-59.72 ± 0.37^{j}	-54.85 ± 0.74^{e}	28.20 ± 0.33^{g}
pH 12		59.72 ± 0.10^{h}	-55.37 ± 0.51^{i}	25.53 ± 0.28^{c}	44.4 ± 0.10^{c}
pH 13		64.84 ± 0.25^{f}	2.25 ± 0.95^{h}	40.27 ± 0.60^{a}	55.49 ± 0.42^{a}
pH 14		59.87 ± 0.38^{h}	5.35 ± 0.77^{g}	37.86 ± 0.22^{b}	53.54 ± 0.31^{b}

[a] Different superscripts in the column indicate significant differences between films in different pH environments at $p < 0.05$.

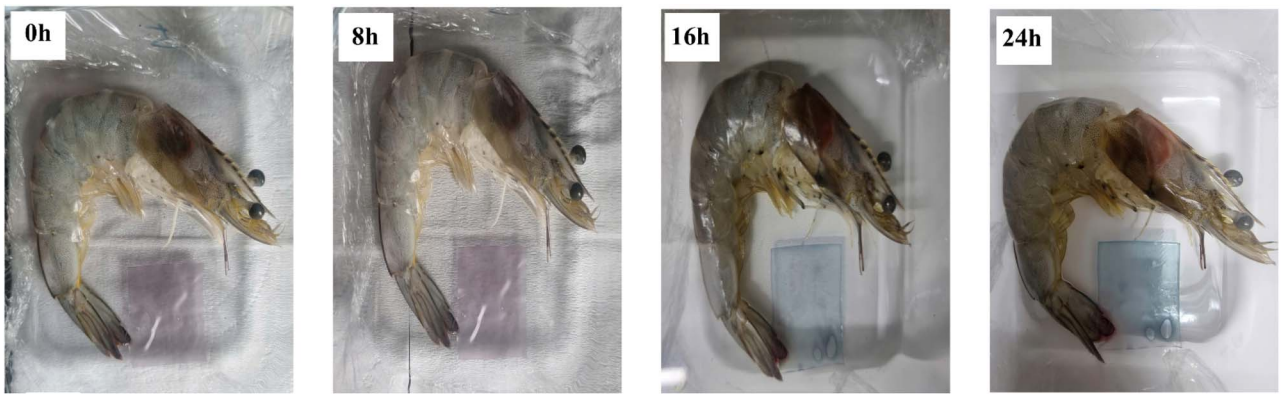

Fig. 10 Color response of bioplastic films containing the anthocyanin extract for real-time monitoring of shrimp freshness at room temperature.

During the decomposition of seafood, especially shrimp, volatile nitrogen compounds such as trimethylamine (TMA), dimethylamine (DMA), and ammonia (NH_3) are produced by the activity of microorganisms and proteolytic enzymes.[76] As the storage time increases, the concentration of these compounds in the surrounding space increases and tends to diffuse into the indicator film. The absorption of these alkaline gases increases the density of hydroxyl ions on the film surface, thereby altering the chemical structure of anthocyanin molecules. Specifically, the conversion to the quinoidal base anion form leads to a color change of the bioplastic film from purple to blue,[85] and the processes are illustrated in Fig. 11. These interesting findings demonstrate the potential application of pH-sensitive films in monitoring the freshness of shrimp as well as other fresh foods during storage.

Limitations

Although the study demonstrated the effectiveness of citric acid as a green hydrolyzing agent to replace mineral acids in cellulose fiber extraction and highlighted the potential application of pH-sensitive bioplastic films, several limitations remain to be addressed. Specifically, the hydrolysis process involved a high citric acid concentration (60% w/w) and a prolonged reaction time (6 hours), which may result in significant energy costs if scaled up for industrial production. In addition, although anthocyanins exhibited a distinct color response to pH changes, the long-term color stability of the film under practical storage conditions, such as exposure to light, oxygen, or high humidity, was not evaluated. These factors may influence the reliability and consistency of the colorimetric signal. Furthermore, the

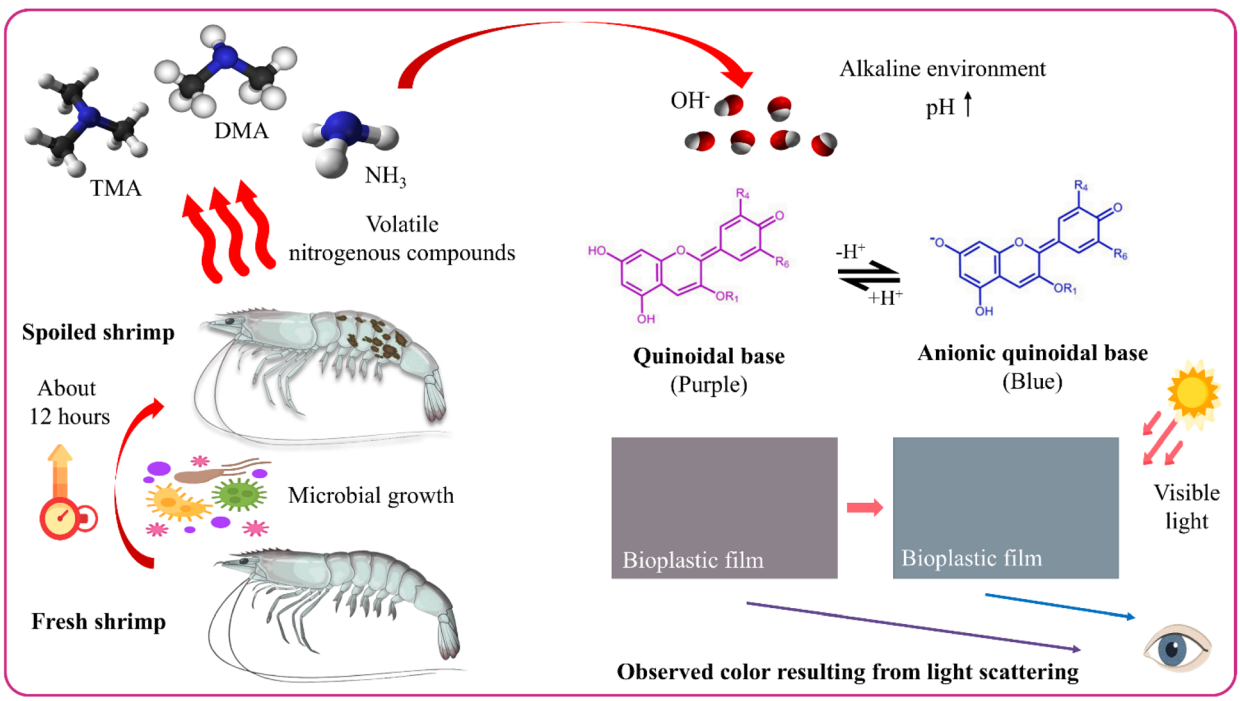

Fig. 11 Mechanism of color change in anthocyanin films during monitoring shrimp freshness.

color change observed during shrimp storage was assessed only qualitatively. Critical quantitative parameters, such as the limit of detection, response time, and the correlation between color intensity and the concentration of volatile compounds, including trimethylamine and ammonia, were not determined. Migration of compounds from the films into food, including overall and specific migration, was also not investigated and should be evaluated in future studies to ensure food safety. Finally, the long-term stability of the film has not been verified, including its storage lifespan and its ability to retain pH-responsive functionality over time, which are essential considerations for potential commercialization.

Conclusion

In this study, a green method was successfully employed to extract cellulose fibers from pineapple crown waste using alkali treatment, hydrogen peroxide bleaching, and citric acid hydrolysis. The obtained cellulose demonstrated a high extraction yield (48.25 ± 0.37%) and a crystallinity index of 78.54%, indicating the effective removal of amorphous components. These fibers were subsequently incorporated into cassava starch films as reinforcement. When 16 wt% cellulose fibers (CFs) were incorporated into the film formulation, the film exhibited significantly enhanced mechanical properties, with a Young's modulus of 318.96 ± 23.24 MPa and a tensile strength of 6.11 ± 0.12 MPa. Furthermore, anthocyanins extracted from purple cabbage were incorporated into the bioplastic film and exhibited excellent color-changing behavior. The bioplastic film labeled CS 0.4 demonstrated enhanced mechanical properties and effective pH-sensing capabilities, suggesting its potential as an intelligent packaging material. Overall, the use of agricultural by-products and natural pigments provided an eco-friendly, promising solution for real-time food freshness monitoring and contributed to advancing sustainable food packaging technologies.

Author contributions

Nguyen Bui Anh Duy: conceptualization; performance of experiments; analysis and interpretation of data; writing – original draft; project administration; investigation. Nguyen Thanh Huy: performance of experiments; analysis and interpretation of data. Bui Phuong Dong: collection of raw materials; analysis and interpretation of data. Pham Nguyen Hong Nhu: assistance in conceptualization; performance of experiments. Phan Quoc Phu: validation; review and editing. Nguyen Chi Thanh: supervision; validation; review and editing.

Conflicts of interest

There are no conflicts to declare.

Data availability

Data supporting this article have been included as part of the supplementary information (SI). Supplementary information: additional characterization results (UV-Vis, tensile test, and color changes). See DOI: https://doi.org/10.1039/d5su00648a.

Acknowledgements

We acknowledge the Ho Chi Minh City University of Technology (HCMUT), VNU-HCM, for supporting this study.

References

1 S. Chen, M. Wu, P. Lu, L. Gao, S. Yan and S. Wang, *Int. J. Biol. Macromol.*, 2020, **149**, 271–280.
2 P. A. V. Freitas, R. R. A. Silva, T. V. de Oliveira, R. R. A. Soares, N. S. Junior, A. R. F. Moraes, A. C. d. S. Pires and N. F. F. Soares, *Lwt*, 2020, **132**, 109780.
3 J. Rajesh Banu and V. Godvin Sharmila, *Sustain. Energy Fuels*, 2023, **7**, 3165–3184.
4 X. Zhang, X. Chen, J. Dai, H. Cui and L. Lin, *Food Packag. Shelf Life*, 2023, **40**, 101215.
5 M. Anwar, M. E. Konnova and S. Dastgir, *RSC Sustain.*, 2025, **3**, 3724–3840.
6 N. N. T. Tien, H. T. Nguyen, N. L. Le, T. T. Khoi and A. Richel, *Food Packag. Shelf Life*, 2023, **37**, 101084.
7 J. R. Westlake, M. W. Tran, Y. Jiang, X. Zhang, A. D. Burrows and M. Xie, *Sustainable Food Technol.*, 2023, **1**, 50–72.
8 Y. Amaregouda and K. Kamanna, *Sustainable Food Technol.*, 2023, **1**, 738–749.
9 M. Meenu, A. K. Pujari, S. Kirar, A. Thakur, M. Garg and J. Bhaumik, *Sustainable Food Technol.*, 2025, **3**, 414–424.
10 Y. Palanisamy, V. Kadirvel and N. D. Ganesan, *Sustainable Food Technol.*, 2025, **3**, 161–180.
11 R. R. Koshy, A. Reghunadhan, S. K. Mary, K. Thomas, A. Kr, S. Thomas and L. A. Pothen, *New J. Chem.*, 2022, **46**, 9036–9047.
12 M. Raji, L. El Foujji, M. E. M. Mekhzoum, M. El Achaby, H. Essabir, R. Bouhfid and A. e. K. Qaiss, *J. Bionic Eng.*, 2022, **19**, 837–851.
13 S. U. Haq, M. Aghajamali and H. Hassanzadeh, *RSC Adv.*, 2021, **11**, 24387–24397.
14 S. K. Mary, R. R. Koshy, J. Daniel, J. T. Koshy, L. A. Pothen and S. Thomas, *RSC Adv.*, 2020, **10**, 39822–39830.
15 L. Prietto, T. C. Mirapalhete, V. Z. Pinto, J. F. Hoffmann, N. L. Vanier, L.-T. Lim, A. R. G. Dias and E. da Rosa Zavareze, *Lwt*, 2017, **80**, 492–500.
16 Q. Gao, R. Ma, L. Shi, S. Wang, Y. Liang and Z. Zhang, *Food Funct.*, 2023, **14**, 2034–2044.
17 S. B. H. Hashim, H. E. Tahir, L. Liu, J. Zhang, X. Zhai, A. A. Mahdi, F. N. Awad, M. M. Hassan, Z. Xiaobo and S. Jiyong, *Food Chem.*, 2022, **373**, 131514.
18 F. Xie, Z. Qin, Y. Luo, Z. He, Q. Chen and J. Cai, *Food Chem.*, 2025, **478**, 143560.
19 A. Ancy, M. Lazar, A. S. Chandran and M. Ushamani, *Sustainable Chem. Pharm.*, 2024, **37**, 101377.
20 B. K. Dejene and T. M. Geletaw, *Polym.-Plast. Technol. Mater.*, 2024, **63**, 540–569.
21 A. Surendren, A. K. Mohanty, Q. Liu and M. Misra, *Green Chem.*, 2022, **24**, 8606–8636.

22 N. Pooja and S. Shashank, *RSC Adv.*, 2024, **14**, 23943–23951.
23 Y. Altynov, K. Bexeitova, M. Nazhipkyzy, S. Azat, A. Konarov, D. Rakhman, N. Sahiner and K. Kudaibergenov, *Nanoscale*, 2025, **17**, 12580–12619.
24 A. A. Reichert, M. R. Sá, T. Castilhos de Freitas, R. Barbosa, T. S. Alves, E. H. Backes, J. H. Alano and A. D. Oliveira, *J. Nat. Fibers*, 2022, **19**, 8541–8554.
25 M. Buvaneswaran, A. Gopan and S. Vr, *Biomass Convers. Biorefin.*, 2025, 1–14.
26 M. Cheng, Z. Qin, J. Hu, Q. Liu, T. Wei, W. Li, Y. Ling and B. Liu, *Carbohydr. Polym.*, 2020, **231**, 115701.
27 S. M. Mohomane, S. V. Motloung, L. F. Koao and T. E. Motaung, *Cellul. Chem. Technol.*, 2022, **56**, 691–703.
28 L. U. S. Faria, B. J. S. Pacheco, G. C. Oliveira and J. L. Silva, *J. Mater. Res. Technol.*, 2020, **9**, 12346–12353.
29 B. Ahmed, J. Gwon, M. Thapaliya, A. Adhikari, S. Ren and Q. Wu, *Cellulose*, 2023, **30**, 2895–2911.
30 C. Liu, H. Du, G. Yu, Y. Zhang, Q. Kong, B. Li and X. Mu, *Pap. Biomater.*, 2017, **2**, 19–26.
31 N. Kaur, P. Chandel, A. J. Capezza, A. Pandey, R. T. Olsson and N. Banik, *RSC Sustain.*, 2025, **3**, 2970–2983.
32 T. J. Bondancia, J. de Aguiar, G. Batista, A. J. G. Cruz, J. M. Marconcini, L. H. C. Mattoso and C. S. Farinas, *Ind. Eng. Chem. Res.*, 2020, **59**, 11505–11516.
33 X. Kang, B. Wang, Y. Ding, L. Xu and Y. Zhang, *Ind. Crops Prod.*, 2024, **219**, 119100.
34 M. S. Wahyudi, H. Bahruji, D. Prasetyoko, A. W. Pratama, D. W. Indriani, L. Suryanegara, R. H. F. Faradilla, M. Mahardika, R. K. Wardani and B. Piluharto, *Case Stud. Chem. Environ. Eng.*, 2025, **11**, 101179.
35 L. A. R. Aisy, T. Kemala, L. Suryanegara and H. Purwaningsih, *Sci. Technol. Indones.*, 2024, **9**, 818–827.
36 N. C. Thanh, N. B. A. Duy, H. T. H. Xuyen, N. T. Huy, B. P. Dong and T. Q. Giang, *Polym. Sci.*, 2024, **66**, 376–386.
37 P. H. F. Pereira, H. L. Ornaghi Jr, V. Arantes and M. O. H. Cioffi, *Carbohydr. Res.*, 2021, **499**, 108227.
38 H. Ji, Z. Xiang, H. Qi, T. Han, A. Pranovich and T. Song, *Green Chem.*, 2019, **21**, 1956–1964.
39 F. W. Hailu, S. W. Fanta, A. A. Tsige and M. A. Delele, *Discov. Sustain.*, 2025, **6**, 1–12.
40 M. Shayan, J. Gwon, M. S. Koo, D. Lee, A. Adhikari and Q. Wu, *Cellulose*, 2022, **29**, 9731–9751.
41 M. L. Hassan, L. Berglund, W. S. Abou Elseoud, E. A. Hassan and K. Oksman, *Cellulose*, 2021, **28**, 10905–10920.
42 J. Ahmed, M. A. Balaji, S. S. Saravanakumar and P. Senthamaraikannan, *J. Nat. Fibers*, 2021, **18**, 1460–1471.
43 J. Chandrasekhar, M. C. Madhusudhan and K. Raghavarao, *Food Bioprod. Process.*, 2012, **90**, 615–623.
44 K. Devarayan and B.-S. Kim, *Sens. Actuators, B*, 2015, **209**, 281–286.
45 M. M. Giusti and R. E. Wrolstad, *Curr. Protoc. Food Anal. Chem.*, 2001, (1), F1.2.1–F1.2.13.
46 K. Pusty, K. K. Dash, A. Tiwari and V. M. Balasubramaniam, *Food Sci. Biotechnol.*, 2023, **32**, 2025–2042.
47 D. Thakur, Y. Kumar, V. S. Sharanagat, T. Srivastava and D. C. Saxena, *Sustainable Chem. Pharm.*, 2023, **36**, 101236.
48 L. Gao, P. Liu, L. Liu, S. Li, Y. Zhao, J. Xie and H. Xu, *Process Biochem.*, 2022, **121**, 463–480.
49 S. Pang, Y. Wang, H. Jia, R. Hao, M. Jan, S. Li, Y. Pu, X. Dong and J. Pan, *Int. J. Biol. Macromol.*, 2023, **230**, 123156.
50 K. Akhila, A. Sultana, D. Ramakanth and K. K. Gaikwad, *Food Biosci.*, 2023, **52**, 102397.
51 C. Rovera, D. Carullo, T. Bellesia, D. Büyüktaş, M. Ghaani, E. Caneva and S. Farris, *Front. Sustain. Food Syst.*, 2023, **6**, 1087867.
52 S. Sihag, J. Pal and M. Yadav, *J. Water Environ. Nanotechnol.*, 2022, **7**, 317–331.
53 K. J. Nagarajan, A. N. Balaji and N. R. Ramanujam, *Int. J. Polym. Anal. Char.*, 2020, **25**, 51–64.
54 A. N. Vu, L. H. Nguyen, H.-C. V. Tran, K. Yoshimura, T. D. Tran, H. Van Le and N.-U. T. Nguyen, *RSC Adv.*, 2024, **14**, 2048–2060.
55 Fitriani, N. A. S. Aprilia and N. Arahman, *IOP Conf. Ser.: Mater. Sci. Eng.*, 2020, **796**, 012007.
56 A. Ganesan and J. Rengarajan, *Iran. Polym. J.*, 2024, **33**, 1157–1170.
57 D. Agarwal, W. MacNaughtan, R. Ibbett and T. J. Foster, *Carbohydr. Polym.*, 2019, **211**, 91–99.
58 M. A. Guancha-Chalapud, L. Serna-Cock and D. F. Tirado, *Appl. Sci.*, 2022, **12**, 6956.
59 P. H. F. Pereira, H. L. Ornaghi Júnior, L. V. Coutinho, B. Duchemin and M. O. H. Cioffi, *Cellulose*, 2020, **27**, 5745–5756.
60 N. A. Kassim, A. Z. Mohamed, E. S. Zainudin, S. Zakaria, S. K. Z. Azman and H. H. Abdullah, *BioResources*, 2019, **14**, 1198–1209.
61 P. H. F. Pereira, V. Arantes, B. Pereira, H. L. Ornaghi Jr, D. M. De Oliveira, S. H. Santagneli and M. O. H. Cioffi, *Cellulose*, 2022, **29**, 8587–8598.
62 F. Fitriani, S. Aprilia, N. Arahman, M. R. Bilad, A. Amin, N. Huda and J. Roslan, *Polymers*, 2021, **13**, 4188.
63 D. Choquecahua Mamani, K. S. Otero Nole, E. E. Chaparro Montoya, D. A. Mayta Huiza, R. Y. Pastrana Alta and H. Aguilar Vitorino, *Recycling*, 2020, **5**, 24.
64 H. A. Silvério, W. P. F. Neto, N. O. Dantas and D. Pasquini, *Ind. Crops Prod.*, 2013, **44**, 427–436.
65 P. Panyamao, S. Charumanee, J. Ruangsuriya and C. Saenjum, *ACS Sustain. Chem. Eng.*, 2023, **11**, 13962–13973.
66 K. S. Prado and M. A. S. Spinacé, *Int. J. Biol. Macromol.*, 2019, **122**, 410–416.
67 L. Q. Dien and T. K. Anh, *J. Jpn. Inst. Energy*, 2021, **100**, 135–143.
68 M. R. K. Sofla, R. J. Brown, T. Tsuzuki and T. J. Rainey, *Adv. Nat. Sci.:Nanosci. Nanotechnol.*, 2016, **7**, 035004.
69 R. K. Punnadiyil, M. P. Sreejith and E. Purushothaman, *J. Chem. Pharm. Sci*, 2016, **974**, 2115.
70 G. P. Bernardes, M. de Prá Andrade and M. Poletto, *J. Mater. Res. Technol.*, 2023, **23**, 64–76.
71 R. M. Vieira, P. B. Sanvezzo, M. C. Branciforti and M. Brienzo, *Bioenergy Res.*, 2023, **16**, 2192–2203.
72 F. Zeng, H. Zeng, Y. Ye, S. Zheng, Y. Zhuang, J. Liu and P. Fei, *Food Funct.*, 2021, **12**, 6821–6829.

73 M. Cheng, X. Yan, Y. Cui, M. Han, X. Wang, J. Wang and R. Zhang, *J. Food Eng.*, 2022, **321**, 110943.
74 H. He, Y. Song, M. Li, H. Zhang, J. Li, H. Huang and Y. Li, *Anal. Methods*, 2023, **15**, 228–239.
75 A. Boonsiriwit, M. Lee, M. Kim, P. Inthamat, U. Siripatrawan and Y. S. Lee, *Food Biosci.*, 2021, **44**, 101392.
76 A. Bouftou, K. Aghmih, D. Belfadil, F. Lakhdar, S. Gmouh and S. Majid, *Food Sci. Biotechnol.*, 2025, **34**, 337–348.
77 M. Alizadeh-Sani, E. Mohammadian, J.-W. Rhim and S. M. Jafari, *Trends Food Sci. Technol.*, 2020, **105**, 93–144.
78 J. Yan, R. Cui, Y. Qin, L. Li and M. Yuan, *Int. J. Biol. Macromol.*, 2021, **177**, 328–336.
79 W. Zhang, X. Li and W. Jiang, *Int. J. Biol. Macromol.*, 2020, **154**, 1205–1214.
80 C. M. P. Yoshida, V. B. V. Maciel, M. E. D. Mendonça and T. T. Franco, *LWT–Food Sci. Technol.*, 2014, **55**, 83–89.
81 M. Shakouri, M. Salami, L.-T. Lim, M. Ekrami, M. Mohammadian, G. Askari, Z. Emam-Djomeh and D. J. McClements, *J. Food Meas. Char.*, 2023, **17**, 472–484.
82 J. L. Li, M. Zhou, G. Cheng, F. Cheng, Y. Lin and P. X. Zhu, *Starch/Staerke*, 2019, **71**, 1800114.
83 M. Lubis, M. B. Harahap, M. H. S. Ginting, M. Sartika and H. Azmi, *J. Eng. Sci. Technol*, 2018, **13**, 381–393.
84 N. A. Azlim, A. Mohammadi Nafchi, N. Oladzadabbasabadi, F. Ariffin, P. Ghalambor, S. Jafarzadeh and A. A. Al-Hassan, *Nutr. Food Sci.*, 2022, **10**, 597–608.
85 K. Zhang, T.-S. Huang, H. Yan, X. Hu and T. Ren, *Int. J. Biol. Macromol.*, 2020, **145**, 768–776.